arXiv:hep-ph/0112164v3 25 Jun 2002

Lepton pair decays of the K_L meson in the light-front model

C. Q. Geng[a,b] and C. W. Hwang[a]

[a] *Department of Physics, National Tsing Hua University, Hsinchu, Taiwan 300, ROC*

[b] *Theory Group, TRIUMF, 4004 Wesbrook Mall, Vancouver, B.C. V6T 2A3, Canada*

Abstract

We analyze K_L lepton pair decays of $K_L \to l^+l^-\gamma$ and $K_L \to l^+l^-l'^+l'^-$ $(l,\, l' = e,\, \mu)$ within the framework of the light-front QCD approach (LFQA). With the $K_L \to \gamma^*\gamma^*$ form factors evaluated in a model with the LFQA, we calculate the decay branching ratios and find out that our results are all consistent with the experimental data. In addition, we study $K_L \to l^+l^-$ decays. We point out that our prediction on $K_L \to e^+e^-$ is about 20% smaller than that in the ChPT. We also discuss whether one could extract the short-distance physics from $K_L \to \mu^+\mu^-$.

PACS numbers: 13.20.Eb, 12.39.Ki

Typeset using REVTEX

I. INTRODUCTION

The study of kaon decays has played a pivotal role in formulating the standard model of electroweak interactions [1]. In particular, the rare decay of $K_L \to \mu^+\mu^-$ was used to constrain the flavor changing neutral current [2] as well as the top quark mass [3]. However, there are ambiguities in extracting the short-distance contribution since the long-distance contribution dominated by the two-photon intermediate state is not well known because its dispersive part cannot be calculated in a reliable way [4–7]. To have a better understanding of this dispersive part, it is important to study the lepton pair decays of the K_L meson such as $K_L \to l^+l^-\gamma$ and $l^+l^-l^+l^-$ $(l = e, \mu)$ since they can provide us with information on the structure of the $K_L \to \gamma^*\gamma^*$ vertex [4–7]. On the other hand, since these lepton pair decays are dominated by the long-distance physics, they can also be served as a testing ground for theoretical techniques such as chiral Lagrangian or other non-perturbative methods that seek to account for the low-energy behavior of QCD.

Recently, several new measurements of the decay branching ratios of $K_L \to \mu^+\mu^-\gamma$, $K_L \to e^+e^-e^+e^-$, and $K_L \to e^+e^-\mu^+\mu^-$ have been reported [8–11]. These decays proceed entirely through the $K\gamma^*\gamma^*$ vertex and provide the best opportunity for the study of its form factor. In Ref. [12], since the assumption of neglecting the momentum dependence for the form factor was adopted, the results for the decays are only valid for those with only the electron-positron pair. In Ref. [13], the decays were studied at the order p^6 in Chiral Perturbation Theory (ChPT). However, all the results in Ref. [13] are smaller than the current experimental values. In this work, we consider another non-perturbative method in the LFQA to analyze the $K\gamma^*\gamma^*$ form factor. As is well known [14], the LFQA allows an exact separation in momentum space between the center-of-mass motion and intrinsic wave functions. A consistent treatment of quark spins and the center-of-mass motion can also be carried out. It has been successfully applied to calculate various form factors [15–18].

The paper is organized as follows. In Sec. II, we derive the theoretical formalism for the decay constant and the $K\gamma^*\gamma^*$ vertex and use these formalism in the LFQA to extract the decay constant and the form factor. In Sec. III, we fix the parameters appearing in the wave functions and calculate the form factors and branching ratios. Finally, conclusions are given in Sec. IV.

II. FRAMEWORK

We start with the K meson decay constant f_K, defined by

$$\langle 0|A^\mu|K(P)\rangle = if_K P^\mu, \tag{2.1}$$

where $A^\mu = \bar{u}\gamma^\mu\gamma_5 s$ is the axial vector current. Assuming a constant vertex function Λ_K [16,27] which is related to the $u\bar{s}$ bound state of the kaon. Then the quark-meson diagram, depicted in Fig. 1 (a), yields

$$\langle 0|A^\mu|K(P)\rangle = -\sqrt{N_c}\int \frac{d^4p_1}{(2\pi)^4}\Lambda_K \mathrm{Tr}\left[\gamma_5 \frac{i(\not{p}_2 + m_s)}{p_2^2 - m_s^2 + i\epsilon}\gamma^\mu\gamma_5 \frac{i(\not{p}_1 + m_u)}{p_1^2 - m_u^2 + i\epsilon}\right], \tag{2.2}$$

where $m_{u,s}$ are the masses of u and s quark, respectively, and N_c is the number of colors. We consider the poles in denominators in terms of the LF coordinates $(p^-, p^+, p_\perp)$ and perform the integration over the LF "energy" p_1^- in Eq. (2.6). The result is

$$\langle 0|A^\mu|K(P)\rangle = \sqrt{N_c}\int \frac{[d^3p_1]}{p_1^+p_2^+}\,\frac{\Lambda_{K_L}}{P^- - p^-_{1\mathrm{on}} - p^-_{2\mathrm{on}}}\,(I_1^\mu|_{p_1^-=p^-_{1\mathrm{on}}}), \tag{2.3}$$

where

$$\begin{aligned} [d^3p_1] &= \frac{dp_1^+d^2p_{1\perp}}{2(2\pi)^3}, \quad p^-_{i\mathrm{on}} = \frac{m_i^2 + p_{i\perp}^2}{p_i^+}, \\ I_1^\mu &= \mathrm{Tr}[\gamma_5(\not{p}_2 + m_s)\gamma^\mu\gamma_5(\not{p}_1 + m_u)]. \end{aligned} \tag{2.4}$$

For $K_L \to \gamma^*\gamma^*$, with the assumption of CP conservation the amplitude is given by

$$A(K_L \to \gamma^*(q_1,\epsilon_1)\;\gamma^*(q_2,\epsilon_2)) = iF(q_1^2,q_2^2)\;\varepsilon_{\mu\nu\rho\sigma}\;\epsilon_1^\mu\;\epsilon_2^\nu\;q_1^\rho\;q_2^\sigma, \tag{2.5}$$

where the form factor of $F(q_1^2,q_2^2)$ in Eq. (2.5) is a symmetric function under the interchange of q_1^2 and q_2^2. In our model, by using the same procedure as above, from the quark-meson diagram depicted in Fig. 2 we get

$$\begin{aligned} A(K_L \to \gamma^*\;\gamma^*) = -\int \frac{d^4p_1}{(2\pi)^4}\Lambda_{K_L}\Bigg\{\mathrm{Tr}\Bigg[\gamma_5\frac{i(\not{p}_3 + m_s)}{p_3^2 - m_s^2 + i\epsilon}\;\not{\epsilon}_2\frac{i(\not{p}_2 + m_s)}{p_2^2 - m_s^2 + i\epsilon} \\ \times C_W(q_1^2)\;\not{\epsilon}_1\frac{i(\not{p}_1 + m_d)}{p_1^2 - m_d^2 + i\epsilon} + (d \leftrightarrow s)\Bigg] + (\epsilon_1 \leftrightarrow \epsilon_2)\Bigg\}, \end{aligned} \tag{2.6}$$

where $p_2 = p_1 - q_1$, $p_3 = p_1 - P$, and C_W is the effective contribution to the inclusive $s \to d\gamma^*$ decay. After integrating over p_1^-, we obtain

$$\begin{aligned} A(K_L \to \gamma^*\;\gamma^*) = \Bigg\{\Bigg[&\int_0^{q_1} \frac{[d^3p_1]}{\prod_{i=1}^3 p_i^+}\frac{\Lambda_{K_L}}{P^- - p^-_{1\mathrm{on}} - p^-_{3\mathrm{on}}}(I_2|_{p_1^-=p^-_{1\mathrm{on}}})\frac{C_W(q_1^2)}{q_1^- - p^-_{1\mathrm{on}} - p^-_{2\mathrm{on}}} \\ &+ \int_{q_1}^{P} \frac{[d^3p_1]}{\prod_{i=1}^3 p_i^+}\frac{\Lambda_{K_L}}{P^- - p^-_{1\mathrm{on}} - p^-_{3\mathrm{on}}}(I_2|_{p_3^-=p^-_{3\mathrm{on}}})\frac{C_W(q_1^2)}{q_2^- - p^-_{2\mathrm{on}} - p^-_{3\mathrm{on}}} + (d \leftrightarrow s)\Bigg] \\ &+ (\epsilon_1 \leftrightarrow \epsilon_2)\Bigg\}, \end{aligned} \tag{2.7}$$

where $q_2^- = P^- - q_1^-$ and

$$I_2 = \mathrm{Tr}[\gamma_5(\not{p}_3 + m_s)\;\not{\epsilon}_2(\not{p}_2 + m_s)\;\not{\epsilon}_1(\not{p}_1 + m_d)]. \tag{2.8}$$

We note that we do not expect that the absolute decay widths of $K_L \to l^+l^-\gamma$ and $K_L \to \gamma\gamma$ calculated from Eq. (2.7) can fit to the experimental values [20]. However, we can estimate the relative form factors of these leptonic decays versus the two-photon decay, and compare the branching ratios with the experimental ones. Recent works on both short-distance (SD) and long-distance (LD) contributions to $s \to d\gamma^*$ can be found in Ref. [21].

As described in Ref. [22], the vertex function Λ_{K_L} and the denominators in Eq. (2.7) correspond to the K_L meson bound state. In the LFQA, the internal structure of the meson bound state [17,18,23] consists of ϕ, which describes the momentum distribution of the constituents in the bound state, and $R^{S,S_z}_{\lambda_1,\lambda_2}$, which creates a state of definite spin (S, S_z) out of LF helicity (λ_1, λ_2) eigenstates and is related to the Melosh transformation [24]. A convenient approach relating these two parts is shown in Ref. [22]. The interaction Hamiltonian is assumed to be $H_I = i\int d^3x\bar{\Psi}\gamma_5\Psi\Phi$ where Ψ is the quark field and Φ is the meson field containing ϕ and $R^{S,S_z}_{\lambda_1,\lambda_2}$. When considering the normalization of the meson state depicted in Fig. 1 (b) in the LFQA, we obtain

$$\begin{aligned}\langle M(P', S', S'_z)|H_I\ H_I|M(P, S, S_z)\rangle &= 2(2\pi)^3\delta^3(P'-P)\delta_{SS'}\delta_{S_zS'_z} \\ &\times \int[d^3p_1]\phi^2 R^{S,S_z}_{\lambda_1,\lambda_2} R^{S',S'_z}_{\lambda_1,\lambda_2}\mathrm{Tr}\left[\gamma_5\frac{-\not{p}_2+m_2}{p_2^+}\gamma_5\frac{\not{p}_1+m_1}{p_1^+}\right].\end{aligned} \tag{2.9}$$

If we normalize the meson state and the momentum distribution function ϕ as [17]

$$\langle M(P', S', S'_z)|H_I\ H_I|M(P, S, S_z)\rangle = 2(2\pi)^3P^+\delta^3(P'-P)\delta_{SS'}\delta_{S_zS'_z}, \tag{2.10}$$

and

$$\int\frac{d^3p_1}{2(2\pi)^3}\frac{1}{P^+}|\phi|^2 = 1, \tag{2.11}$$

respectively, where p_1 and p_2 are the on-mass-shell momenta, we have that

$$R^{S,S_z}_{\lambda_1,\lambda_2} = \frac{\sqrt{p_1^+p_2^+}}{2\sqrt{p_{1\mathrm{on}}\cdot p_{2\mathrm{on}}+m_1m_2}}. \tag{2.12}$$

The wave function and the Melosh transformation of the meson are related to the bound state vertex function Λ_M by

$$\frac{\Lambda_M}{P^- - p^-_{1\mathrm{on}} - p^-_{2\mathrm{on}}} \longrightarrow R^{S,S_z}_{\lambda_1,\lambda_2}\ \phi_M\,. \tag{2.13}$$

We note that p_1, p_2 and p_3 in the trace of $I_{1,2}$ must be on the mass shell for self-consistency. After taking the "good " component $\mu = +$, we use the definitions of the LF momentum variables $(x, x', k_\perp, k'_\perp)$ [18] and take a Lorentz frame where $P_\perp = P'_\perp = 0$ to have $q_\perp = 0$ and $k'_\perp = k_\perp$. The decay constant f_K and the form factor $F(q_1^2, q_2^2)$ can be extracted by comparing these results with Eqs. (2.1) and (2.5), respectively, *i.e.*,

$$f_K = 2\sqrt{2}\sqrt{N_c}\int\frac{dx\,d^2k_\perp}{2(2\pi)^3}\frac{\phi_{K_L}(x,k_\perp)}{\sqrt{a^2+k_\perp^2}}\,a\,, \tag{2.14}$$

and

$$\begin{aligned}F(q_1^2, q_2^2) = \int\frac{d^2k_\perp}{2(2\pi)^3}\Bigg\{C_W(q_1^2)\Bigg[\int_0^{r_+}dx\ &\frac{\phi_{K_L}(x,k_\perp)}{\sqrt{a^2+k_\perp^2}}\frac{a[r_+/(r_+-x)]}{\frac{m_s^2+k_\perp^2}{(x/r_+)}+\frac{m_s^2+k_\perp^2}{1-(x/r_+)}-q_2^2} \\ +\int_{r_+}^1 dx\ &\frac{\phi_{K_L}(x,k_\perp)}{\sqrt{a^2+k_\perp^2}}\frac{a[(1-r_+)/(x-r_+)]}{\frac{m_d^2+k_\perp^2}{(1-x)/(1-r_+)}+\frac{m_s^2+k_\perp^2}{(x-r_+)/(1-r_+)}-q_1^2}+(d\leftrightarrow s)\Bigg] \\ +(q_1\leftrightarrow q_2; r_+\leftrightarrow 1-r_-)\Bigg\},\end{aligned} \tag{2.15}$$

where

$$a = m_{u,d}x + m_s(1-x)\,, \quad m_u \; = \; m_d\,,$$
$$r_\pm = \frac{1}{2M_{K_L}^2}[M_{K_L}^2 + q_1^2 - q_2^2 \pm \sqrt{(M_{K_L}^2 + q_1^2 - q_2^2)^2 - 4M_{K_L}^2 q_1^2}\ ], \tag{2.16}$$

and x is the momentum fraction carried by the spectator antiquark in the initial state.

In principle, the momentum distribution amplitude $\phi(x, k_\perp)$ can be obtained by solving the LF QCD bound state equation [25]. However, before such first-principle solutions are available, we shall have to use phenomenological amplitudes. One momentum distribution function that has often been used in the literature for mesons is the Gaussian-type,

$$\phi(x, k_\perp)_{\mathrm{G}} = \mathcal{N}\sqrt{\frac{dk_z}{dx}}\ \exp\left(-\frac{\vec{k}^2}{2\omega^2}\right)\,, \tag{2.17}$$

where $\mathcal{N} = 4(\pi/\omega^2)^{3/4}$ and k_z is of the internal momentum $\vec{k} = (\vec{k}_\perp, k_z)$, defined through

$$1 - x = \frac{e_1 - k_z}{e_1 + e_2}, \qquad x = \frac{e_2 + k_z}{e_1 + e_2}, \tag{2.18}$$

with $e_i = \sqrt{m_i^2 + \vec{k}^2}$. We then have

$$M_0 = e_1 + e_2, \qquad k_z = \frac{xM_0}{2} - \frac{m_2^2 + k_\perp^2}{2xM_0}, \tag{2.19}$$

and

$$\frac{dk_z}{dx} = \frac{e_1 e_2}{x(1-x)M_0}, \tag{2.20}$$

which is the Jacobian of the transformation from $(x, k_\perp)$ to $\vec{k}$.

III. NUMERICAL RESULTS

To examine numerically the form factor derived in Eq. (2.15), we need to specify the parameters appearing in $\phi_M(x, k_\perp)$. To fit the meson masses, in Ref. [26] $m_u = 0.22(0.25)$ GeV and $m_s = 0.45(0.48)$ GeV are obtained with some interaction potentials, while in Ref. [27] $m_u = 0.25$ GeV and $m_s = 0.37$ GeV in the invariant meson mass scheme. Here we do not consider any potential form and scheme and just use the decay constant $f_K = 159.8$ MeV [28], charge radius $\langle r^2\rangle_K = 0.34\ \mathrm{fm}^2$ [29], and the quark masses of $m_{u,d}$ to constrain the s quark mass of m_s and the scale parameter of ω in Eq. (2.17). By using $m_u = m_d = 250$ MeV [18], we find that $m_s = 400$ MeV and $\omega = 0.38$ GeV. We note that the lower mass of m_s should not affect the meson masses once we choose a suitable potential [26] or scheme [27]. Now, we use the momentum distribution functions $\phi(x, k_\perp)_{\mathrm{G}}$ to calculate the form factors $F(q_1^2, q_2^2)$ in time-like region of $0 \le q_1^2$ and $q_2^2 \le M_K^2 \simeq 0.25\ \mathrm{GeV}^2$. In this low energy region, we neglect the momentum dependence of the effective vertex $C_W(q^2)$ in Eq. (2.15), that is,

$$C_W(q^2) \simeq C_W(0). \tag{3.1}$$

We can use Eqs. (2.15) and (3.1) to get the function $f(y) \equiv F(q_1^2, 0)/F(0,0)$, where $y \equiv q_1^2/M_K^2$, and the result for $|f(y)|^2$ is shown in Fig. 3. From the figure, we see that our result with the assumption of Eq. (3.1) agrees well with experimental data [30–32], especially in the lower y region. To get a better fit for a larger y, we may use

$$C_W(q^2) \simeq \frac{C_W(0)}{(1-\frac{q^2}{m_c^2})^n}\,. \tag{3.2}$$

As seen from Fig. 3, we find that the fit for $n\,(<8)$ is better than that for $n-1$. In particular, a larger value of n is preferred if we disregard the data from E845 at BNL [31] in Fig. 3. The experimental result on $K_L \to \mu^+\mu^-\gamma$ from NA48 at CERN, which is currently being analyzed [33], should help to resolve this matter. To illustrate our results on the lepton pair decays, we shall take $n = 0$ and 3, referring as (I) and (II), respectively.

The function of $f(y)$ is related to the differential decay rate of $K_L^0 \to l^+l^-\gamma$ by

$$\frac{d\mathcal{B}_{l^+l^-\gamma}}{dq_1^2} \equiv \frac{d\,\Gamma(K_L \to l^+l^-\,\gamma)}{\Gamma(K_L \to \gamma\gamma)\,dq_1^2} = \frac{2}{q_1^2}\left(\frac{\alpha}{3\pi}\right)|f(y)|^2\,\lambda^{3/2}\left(1, \frac{q_1^2}{M_{K_L}^2}, 0\right)\,G_l(q_1^2), \tag{3.3}$$

where

$$\lambda(a,b,c) = a^2 + b^2 + c^2 - 2(ab + bc + ca), \tag{3.4}$$

and

$$G_l(q^2) = \left(1 - \frac{4\,M_l^2}{q^2}\right)^{1/2}\left(1 + \frac{2\,M_l^2}{q^2}\right). \tag{3.5}$$

Integrating over q_1^2 in Eq. (3.3), we get the branching ratios

$$\begin{aligned}\mathcal{B}_{e^+e^-\gamma} &\equiv \frac{\Gamma(K_L^0 \to e^+e^-\gamma)}{\Gamma(K_L^0 \to \gamma\gamma)} = 1.64\,,\ 1.65 \times 10^{-2},\\ \mathcal{B}_{\mu^+\mu^-\gamma} &\equiv \frac{\Gamma(K_L^0 \to \mu^+\mu^-\gamma)}{\Gamma(K_L^0 \to \gamma\gamma)} = 5.50\,,\ 6.20 \times 10^{-4},\end{aligned} \tag{3.6}$$

for (I) and (II), respectively. These values agree well with the experimental data: $\mathcal{B}^{\rm exp}_{e^+e^-\gamma} = (1.69 \pm 0.13) \times 10^{-2}$ [28] and $\mathcal{B}^{\rm exp}_{\mu^+\mu^-\gamma} = (6.11 \pm 0.31) \times 10^{-4}$ [8], where we have used [34]

$$\Gamma^{\rm exp}(K_L^0 \to \gamma\gamma) = [(5.92 \pm 0.15) \times 10^{-4}]\Gamma^{\rm exp}(K_L^0 \to \text{all}). \tag{3.7}$$

On the other hand, our results are larger than $\mathcal{B}_{e^+e^-\gamma} = 1.59\times10^{-2}$ and $\mathcal{B}_{\mu^+\mu^-\gamma} = 4.09\times10^{-4}$, respectively, obtained in Ref. [12], where the momentum dependence of the form factor was neglected, i.e., $f(y) = 1$. This inconsistency is reasonable because the kinematic factor $G_l(q^2)$ which leads the contribution at $q^2 \simeq 4M_l^2$ is important, and the electron mass is very small so that $f(y) = 1$ is only valid for the decay with an electron-positron pair. For the muonic pair case, since the mass of muon is not small, the effect of the deviation of neglecting the momentum dependence is evident. This situation also occurs in the decays with two lepton pairs.

Next, Eq. (2.15) can be also used to calculate the differential decay rates of $K_L \to l^+l^-l'^+l'^-$ by

$$\frac{d\,\Gamma(K_L \to l^+l^-l'^+l'^-)}{\Gamma(K_L \to \gamma\gamma)\, dq_1^2\, dq_2^2} = \frac{2}{q_1^2 q_2^2} \left(\frac{\alpha}{3\pi}\right)^2 \left|\frac{F(q_1^2, q_2^2)}{F(0,0)}\right|^2 \lambda^{3/2} \left(1, \frac{q_1^2}{M_{K_L}^2}, \frac{q_2^2}{M_{K_L}^2}\right) G_l(q_1^2)\, G_{l'}(q_2^2). \quad (3.8)$$

After the integrations over q_1^2 and q_2^2, for (I) and (II) we obtain the branching ratios as follows:

$$\begin{aligned}
\mathcal{B}_{e^+e^-e^+e^-} &\equiv \frac{\Gamma(K_L^0 \to e^+e^-e^+e^-)}{\Gamma(K_L^0 \to \gamma\gamma)} = 6.61\,,\ 6.74 \times 10^{-5}, \\
\mathcal{B}_{\mu^+\mu^-e^+e^-} &\equiv \frac{\Gamma(K_L^0 \to \mu^+\mu^-e^+e^-)}{\Gamma(K_L^0 \to \gamma\gamma)} = 3.87\,,\ 4.37 \times 10^{-6}, \\
\mathcal{B}_{\mu^+\mu^-\mu^+\mu^-} &\equiv \frac{\Gamma(K_L^0 \to \mu^+\mu^-\mu^+\mu^-)}{\Gamma(K_L^0 \to \gamma\gamma)} = 1.50\,,\ 1.73 \times 10^{-9}. \qquad (3.9)
\end{aligned}$$

In Table 1, we summary the experimental and theoretical values of the decay branching ratios for the K_L lepton pair modes. The results of Ref. [12] correspond a point-like form factor, while those in Ref. [13] are calculated at $O(p^6)$ in the ChPT.

Table 1: Summary of the lepton pair decays of K_L.

Br	PDG [28]	new data	(I)	(II)	Ref. [12]	Ref. [13]
$10^2 \times \mathcal{B}_{e^+e^-\gamma}$	1.69 ± 0.09		1.64	1.65	1.59	1.60 ± 0.15
$10^4 \times \mathcal{B}_{\mu^+\mu^-\gamma}$	5.49 ± 0.49	6.11 ± 0.31 [8]	5.50	6.20	4.09	4.01 ± 0.57
$10^5 \times \mathcal{B}_{e^+e^+e^-e^-}$	6.93 ± 0.20	6.28 ± 0.65 [9] 6.20 ± 0.69 [10]	6.61	6.74	5.89	6.50
$10^6 \times \mathcal{B}_{\mu^+\mu^-e^+e^-}$	$4.9^{+11.3}_{-4.0}$	4.43 ± 0.84 [11]	3.87	4.37	1.42	2.20 ± 0.25
$10^9 \times \mathcal{B}_{\mu^+\mu^-\mu^+\mu^-}$			1.50	1.73	0.946	1.30 ± 0.15

From Table 1, we may also combine the experimental values by assuming that they are uncorrelated and we find that

$$\begin{aligned}
\mathcal{B}^{\text{exp}}_{K_L\to\mu^+\mu^-\gamma} &= (5.93 \pm 0.26) \times 10^{-4}\,, \\
\mathcal{B}^{\text{exp}}_{K_L\to e^+e^-e^+e^-} &= (6.83 \pm 0.19) \times 10^{-5}\,, \\
\mathcal{B}^{\text{exp}}_{K_L\to\mu^+\mu^-e^+e^-} &= (4.44^{+0.84}_{-0.82}) \times 10^{-6}\,. \qquad (3.10)
\end{aligned}$$

It is interesting to see that our results for $K_L \to l^+l^-\gamma$ are larger than those in Refs. [12,13] and agree very well with the experimental data. Furthermore, as shown in Eq. (3.9), those for $K_L \to e^+e^-e^+e^-$ and $K_L \to \mu^+\mu^-e^+e^-$ also agree with the combined experimental values in Eq. (3.10). Here, we do not consider the interference effect [12,13] from the identical leptons in the final state. The reasons are given in the following. When we use the non-point-like form factor, this effect is about 0.5% in the $e^+e^-e^+e^-$ mode [13], which is beyond experimental access. For the $\mu^+\mu^-\mu^+\mu^-$ mode, the relative size of the interference effect is larger, but it is outside the scope of future experiments because the total branching ratio is predicted to be about 8×10^{-13}.

We now use the form factor $F(q_1^2, q_2^2)$ to calculate the decays of $K_L \to l^+l^-$. The decay branching ratios of the modes can be generally decomposed in the following way

$$\mathcal{B}_{l^+l^-} \equiv \frac{\Gamma(K_L \to l^+l^-)}{\Gamma(K_L \to \gamma\gamma)} = |\mathrm{Im}\ \mathcal{A}_l|^2 + |\mathrm{Re}\ \mathcal{A}_l|^2, \tag{3.11}$$

where $\mathrm{Im}\,\mathcal{A}_l$ denotes the absorptive contribution and $\mathrm{Re}\,\mathcal{A}_l$ the dispersive one. The former can be determined in a model-independent form of

$$|\mathrm{Im}\ \mathcal{A}_l|^2 = \frac{\alpha^2 M_l^2}{2\,M_{K_L}^2 \beta_l} \left[\ln\frac{1-\beta_l}{1+\beta_l}\right]^2, \tag{3.12}$$

where $\beta_l^2 \equiv 1 - 4M_l^2/M_{K_L}^2$. The latter, however, can be rewritten as the sum of SD and LD contributions,

$$\mathrm{Re}\ \mathcal{A}_l = \mathrm{Re}\ \mathcal{A}_{l\,\mathrm{SD}} + \mathrm{Re}\ \mathcal{A}_{l\,\mathrm{LD}}. \tag{3.13}$$

In the standard model, the SD part has been identified as the weak contribution represented by one-loop W-box and Z-exchange diagrams [3,35,36], while the LD one is related to $F(q_1^2, q_2^2)$ by

$$|\mathrm{Re}\ \mathcal{A}_{l\,\mathrm{LD}}|^2 = \frac{2\alpha^2 M_l^2 \beta_l}{\pi^2 M_{K_L}^2} |\mathrm{Re}\ \mathcal{R}_l(M_{K_L}^2)|^2, \tag{3.14}$$

where [37]

$$\mathcal{R}_l(P^2) = \frac{2i}{\pi^2 M_K^2} \int d^4q \frac{[P^2q^2 - (P\cdot q)^2]}{q^2\,(P-q)^2\,[(q-p_l)^2 - M_l^2]} \frac{F(q^2,(P-q)^2)}{F(0,0)}. \tag{3.15}$$

In general, an once-subtracted dispersion relation can be written for $\mathrm{Re}\,\mathcal{R}$ as [38]

$$\mathrm{Re}\ \mathcal{R}_l(P^2) = \mathrm{Re}\ \mathcal{R}_l(0) + \frac{P^2}{\pi}\int_0^\infty dP'^2 \frac{\mathrm{Im}\ \mathcal{R}_l(P'^2)}{(P'^2-P^2)P'^2}, \tag{3.16}$$

where $\mathrm{Re}\,\mathcal{R}_\mathrm{l}(0)$ can be obtained by applying Eq. (2.15) in the soft limit of $P \to 0$.

For the $K_L \to e^+e^-$ decay, with $n = 0$ and 3 of (I) and (II) in Eq. (3.2) we find that

$$|\mathrm{Re}\ \mathcal{A}_{e\,\mathrm{LD}}|^2 = 5.60\,,\ 6.52 \times 10^{-9}\,, \tag{3.17}$$

respectively. Since the SD part of $\mathrm{Re}\,\mathcal{A}_{\mathrm{e\,SD}}$ can be neglected, we get

$$\begin{aligned} \mathcal{B}^I_{e^+e^-} &= 1.09 \times 10^{-8}\,, \\ \mathcal{B}^{II}_{e^+e^-} &= 1.18 \times 10^{-8}\,, \end{aligned} \tag{3.18}$$

where we have used $|\mathrm{Im}\,\mathcal{A}_\mathrm{e}|^2 = 5.32 \times 10^{-9}$. In terms of the total decay branching ratio $B_{e^+e^-} = \Gamma(K_L \to e^+e^-)/\Gamma(K_L \to all)$, the numbers in Eq. (3.18) are about 6.5 and 7.0×10^{-12}, respectively. Both results in Eq. (3.18) are consistent with the experimental value of $\mathcal{B}^{\rm exp}_{e^+e^-} = (1.5^{+1.0}_{-0.7}) \times 10^{-8}$ measured by E871 at BNL [39], but they are lower than the value of $(1.52 \pm 0.09) \times 10^{-8}$ $[B_{e^+e^-} = (9.0 \pm 0.5) \times 10^{-12}]$ given by the calculation in Ref. [5] with the ChPT. It is interesting to note that $\mathcal{B}_{e^+e^-}$ slowly increases as n and reaches 1.22×10^{-8} for $n = 10$. Clearly, our prediction is about 20% smaller than that in the ChPT [5].

For the $K_L \to \mu^+\mu^-$ decay, by subtracting between the value of $|{\rm Im}\,\mathcal{A}_\mu|^2 = 1.20 \times 10^{-5}$ from the experimental data of $\mathcal{B}^{\rm exp}_{\mu^+\mu^-} = (1.21 \pm 0.04) \times 10^{-5}$ [28,40], we obtain that

$$|{\rm Re}\ \mathcal{A}_\mu|^2 \leq 7.2 \times 10^{-7} \quad (90\%\ C.L.). \tag{3.19}$$

In the standard model, we have that [7,41]

$$|{\rm Re}\ \mathcal{A}_{\mu\,{\rm SD}}|^2 \mathcal{B}_{K_L\to\gamma\gamma} = 0.9 \times 10^{-9} (1.2 - \bar{\rho})^2 \left[\frac{\bar{m}_t(m_t)}{170\ {\rm GeV}}\right]^{3.1} \left[\frac{|V_{cb}|}{0.040}\right]^4 , \tag{3.20}$$

where $\bar{\rho} = \rho(1 - \lambda^2/2)$. Using the parameters of $\bar{m}_t(m_t) = 166$ GeV, $|V_{cb}| = 0.041$ and $\bar{\rho} \simeq 0.224$ [36,42], from Eqs. (3.7) and (3.20) we get

$${\rm Re}\ \mathcal{A}_{\mu\,{\rm SD}} \simeq -1.22 \times 10^{-3} , \tag{3.21}$$

which is larger than the limit in Eq. (3.19). It is clear that the value of ${\rm Re}\,\mathcal{A}_{\mu\,{\rm LD}}$ has to be either very small for the same sign as ${\rm Re}\,\mathcal{A}_{\mu\,{\rm SD}}$ or the same order but the opposite sign.

For the case of (I), from Eq. (3.16) we find

$${\rm Re}\ \mathcal{A}^{I}_{\mu\,{\rm LD}} = -1.11 \times 10^{-3} , \tag{3.22}$$

which is very close to the SD value in Eq. (3.21) and clearly ruled out if the absolute sign in Eqs. (3.21) and (3.22) are the same. However, if the relative sign is opposite, the limit in Eq. (3.19) can be satisfied for certain values of ρ. From Eqs. (3.20), (3.19), and (3.22), by taking $\bar{m}_t(m_t) = 166$ GeV and $|V_{cb}| = 0.041$ we extract that

$$\bar{\rho} > -0.37 \ \ \text{or} \ \ \rho > -0.38 \ \ (90\%\, C.L.) . \tag{3.23}$$

We note that the limit in Eq. (3.23) is close to that in Eq. (41) of Ref. [7]. This result is not surprising. If we fit $F(q_1^2, q_2^2)$ in Eq. (2.15) with Eq. (14) of Ref. [7] given by

$$f(q_1^2, q_2^2) = \frac{F(q_1^2, q_2^2)}{F(0,0)} = 1 + \alpha \left(\frac{q_1^2}{q_1^2 - m_\rho^2} + \frac{q_2^2}{q_2^2 - m_\rho^2}\right) + \beta \frac{q_1^2 q_2^2}{(q_1^2 - m_\rho^2)(q_2^2 - m_\rho^2)} , \tag{3.24}$$

we find that $\alpha \simeq -0.585$ and $\beta \simeq 0.191$ and thus

$$1 + 2\alpha + \beta = 2.16 \times 10^{-2} \simeq 0 , \tag{3.25}$$

which satisfies the bound of Eq. (35) in Ref. [7]. Similarly, for (II) we obtain

$${\rm Re}\ \mathcal{A}^{II}_{\mu\,{\rm LD}} = -1.38 \times 10^{-4} . \tag{3.26}$$

It is very interesting to see that the value in Eq. (3.26) is much smaller than ${\rm Re}\,\mathcal{A}_{\mu SD}$ in Eq. (3.21), which is exactly the case discussed in Ref. [3]. From Eq. (3.26), with the same parameters as (I), we find that

$$\bar{\rho} > 0.63,\ 0.41 \quad \text{or} \quad \rho > 0.65,\ 0.42 \quad (90\%\, C.L.) \tag{3.27}$$

for the same and opposite signs between $\mathrm{Re}\,\mathcal{A}_{\mu SD}$ and $\mathrm{Re}\,\mathcal{A}^{II}_{\mu \mathrm{LD}}$, respectively. We note that the limits in Eq. (3.27) do not agree with the recent global fitted value of $\bar{\rho} = 0.224 \pm 0.038$ [36,42], which may not be unexpected since (i) we have not included various possible ranges of $\bar{m}_t(m_t)$, $|V_{cb}|$, and quark masses in the calculation and (ii) we still need to fix n in Eq. (3.2) and modify the form of $C_W(q^2)$ [43]. However, the important message here is that the LD dispersive contribution in $K_L \to \mu^+\mu^-$ is calculable in the LFQA. From our preliminary results, it seems that $\mathrm{Re}\mathcal{A}_{\mu LD}$ is indeed small as anticipated many years ago in Ref. [3]. Moreover, our approach here provides another useful tool for the decays beside the ChPT.

IV. CONCLUSIONS

In this work, we have studied the K_L lepton pair decays of $K_L \to l^+l^-\gamma$ and $K_L \to l^+l^-l'^+l'^-$ in the light-front QCD framework. In our calculations, we have adopted the Gaussian-type wave function and assumed the form of the effective vertex $C_W(q^2)$ in Eq. (3.2) to account for the momentum dependences in the low energy region. We have calculated the relative form factors of the leptonic decays vs. the two-photon decay, and have showed that our results on the decay branching ratios of $K_L \to l^+l^-\gamma$ and $e^+e^-l^+l^-$ $(l = e, \mu)$ agree well with the experimental data. The remarkable agreements indicate that our form for $C_W(q^2)$ is quite reasonable, but the number of n still needs to be fixed. Furthermore, all our predicted values for these decays are larger than those in the ChPT [12,13], in particular for the modes of $\mu^+\mu^-\gamma$ and $\mu^+\mu^-e^+e^-$ for which the $O(p^6)$ ChPT results in Ref. [13] are ruled out by the new experimental data [8,11]. On the other hand, for $K_L \to e^+e^-$, we have found that $\mathcal{B}_{e^+e^-}$ is between 1.09 and 1.22×10^{-8} for $n = (0, 10)$, which are lower than $(1.52 \pm 0.09) \times 10^{-8}$ in the ChPT [5]. For $K_L \to \mu^+\mu^-$, we have demonstrated that the long-distance dispersive contribution is possibly small. However, to get a meaningful constraint on the CKM parameters, further theoretical studies [43] as well as more precise experimental data such as those from NA48 at CERN [33] on the spectra of the pair decays are needed. Finally, we remark that our approach cannot calculate the absolute decay widths of $K_L \to l^+l^-\gamma$ and $K_L \to \gamma\gamma$.

ACKNOWLEDGMENTS

We would like to thank K. Terasaki for useful data. This work was supported in part by the National Science Council of R.O.C. under the Grant No. NSC90-2112-M-007-040.

REFERENCES

[1] For a review, see L.Littenberg and G.Valencia, Annu. Rev. Nucl. Part. Sci. **43**, 729 (1993).

[2] S.L. Glashow, J. Iliopoulos and L. Maiani, Phys. Rev. **D 2**, 1585 (1973); M.K. Gaillard and B.W. Lee, Phys. Rev. **D 10** 897 (1974), M.K. Gaillard, B.W. Lee and R.E. Shrock, Phys. Rev. **D 13**, 2674 (1976); R.E. Shrock and M.B. Voloshin, Phys. Lett. **B 87**, 375 (1979).

[3] A.J. Buras, Phys. Rev. Lett. **46**, 1354(1981); L. Bergstrom, E. Masso, P. Singer, and D. Wyler, Phys. Lett. **B 134**, 373 (1984); C.Q. Geng and J.N. Ng, Phys. Rev. **D 41**, 2351 (1990).

[4] L. Bergstrom, E. Masso, and P. Singer, Phys. Lett. **B 249**, 141 (1990); G. Bélanger and C.Q. Geng, Phys. Rev. **D 43**, 140 (1991); L. Ritchie and S.G. Wojcicki, Rev. Mod. Phys. 65, 1149 (1993); L. Littenberg and G. Valencia, Annu. Rev. Nucl. Part. Sci. **43** 729 (1993).

[5] G. Valencia, Nucl. Phys. **B 517**, 339 (1998).

[6] J.O. Eeg, K. Kumericki and I. Picek, hep-ph/9605337; D. Gomez Dumm and A. Pich, Phys. Rev. Lett. **80**, 4633 (1998); M. Knecht, S. Peris, M. Perrottet, and E. de Rafael, Phys. Rev. Lett. **83**, 5230 (1999).

[7] G. D'Ambrosio, G. Isidori, and J. Portoles, Phys. Lett. **B 423**, 385 (1998).

[8] A. Alavi-Harati, *et al.* (KTeV Collaboration), Phys. Rev. Lett. **87**, 071801 (2001).

[9] A. Alavi-Harati, *et al.* (KTeV Collaboration), Phys. Rev. Lett. **86**, 5425 (2001).

[10] A. Lai, *et al.* (NA48 Collaboration), hep-ex/0006040.

[11] A. Alavi-Harati, *et al.* (KTeV Collaboration), Phys. Rev. Lett. **87**, 111802 (2001).

[12] T. Miyazaki and E. Takasugi, Phys. Rev. **D 8**, 2051 (1973).

[13] L. Zhang and J.L. Goity, Phys. Lett. **B 398**, 387 (1997); L. Zhang and J.L. Goity, Phys. Rev. **D 57**, 7031 (1998).

[14] For a review, see B.D. Ksister and W.N. Polyzou, Adv. Nucl. Phys. **20**, 225 (1991); F. Coester, Progress in Part. and Nucl. Phys. **29**, 1 (1992).

[15] F. Cardarelli, *et al.*, Phys. Rev. **D 53**, 6682 (1996); P.J. O'Donnell, *et al.*, Phys. Lett. **B 325**, 219 (1994);

[16] N.B. Demchuk *et al.*, Phys. Atom. Nucl **59**, 2152 (1996).

[17] C.Y. Cheung, C.W. Hwang, and W.M. Zhang, Z. Phys. **C 75**, 657 (1997).

[18] H.Y. Cheng, C.Y. Cheung, and C.W. Hwang, Phys. Rev. **D 55**, 1559 (1997)

[19] W. Jaus, Phys. Rev. **D 41**, 3394 (1990); *ibid.* **D 44**, 2851 (1991); Z. Phys. **C 54**, 611 (1992).

[20] F.J. Gilman and M.B. Wise, Phys. Rev. **D 19**, 976, (1979).

[21] G. Eilam *et al.*, Phys. Rev. **D 53**, 3629 (1996); X.G. He and G. Valencia, Phys. Rev. **D 61**, 075003, (2000); J. Tandean, Phys. Rev. **D 61**, 114022, (2000); and references therein.

[22] C.W. Hwang, Phys. Lett. **B 530**, 93 (2002).

[23] C.W. Hwang, Phys. Rev. **D 64**, 034011 (2001).

[24] H.J. Melosh, Phys. Rev. **D 9**, 1095 (1974).

[25] W. M. Zhang, Chin. J. Phys. **31**, 717 (1994); hep-ph/9510428.

[26] H.M. Choi and C.R. Ji, Phys. Rev. **D 59**, 074015 (1999).

[27] W. Jaus, Phys. Rev. **D 44**, 2851 (1991).

[28] D.E. Groom, *et al.* (Particle Data Group), Eur. Phys. J. **C 15**, 1 (2000).
[29] S.R. Amendolia *et al.*, Phys. Lett. **B 178**, 435 (1986).
[30] E799 Collaboration, N.B. Spencer, *et al.*, Phys. Rev. Lett. **74**, 3323 (1995).
[31] E845 Collaboration, K.E. Ohl, *et al.*, Phys. Rev. Lett. **65**, 1407 (1990).
[32] NA31 Collaboration, C.D. Barr, *et al.*, Phys. Lett. **B 240**, 283 (1990).
[33] H. Wahl, private communications.
[34] Burkhardt H *et al.*, Phys. Lett. **B 199**, 139 (1987).
[35] T. Inami and C. S. Lim, Prog. Theor. Phys. **65**, 297 (1981).
[36] For a recent review, see A.J. Buras, hep-ph/0101336.
[37] Ll. Ametller, A. Bramon, E. Massó, Phys. Rev. **D 48**, 3388 (1993).
[38] L. Bergström, *et al.*, Phys. Lett. **B 126**, 117 (1983).
[39] D. Ambrose *et al.*, E871 Collabration, Phys. Rev. Lett. **81**, 4309 (1998).
[40] D. Ambrose *et al.*, E871 Collabration, Phys. Rev. Lett. **84**, 1389 (2000).
[41] G. Buchalla and A.J. Buras, Nucl. Phys. **B412**, 106 (1996); A.J. Buras and R. Fleischer, hep-ph/9704376.
[42] M. Ciuchini *et al.*, JHEP **0107**, 013 (2001), hep-ph/0012308.
[43] C.Q. Geng and C.W. Hwang, in progress.

FIGURE CAPTIONS

Fig. 1 Feynman diagrams for the meson (a) decay constant and (b) normalization.

Fig. 2 Feynman triangle diagrams with (a) and (b) corresponding to the LF valence configuration. Empty circles indicate LF wave functions.

Fig. 3 The y-dependent behavior of $|f(y)|^2$, where the lines from bottom to top corresponding to $n = 0, 1, \cdots, 10$ are obtained by this work with $f_K = 159.8$MeV and $m_s = 400$MeV and the experimental data are taken from E799 at FNAL [30], E845 at BNL [31], and NA31 at CERN [32], respectively.

FIGURES

FIG. 1.

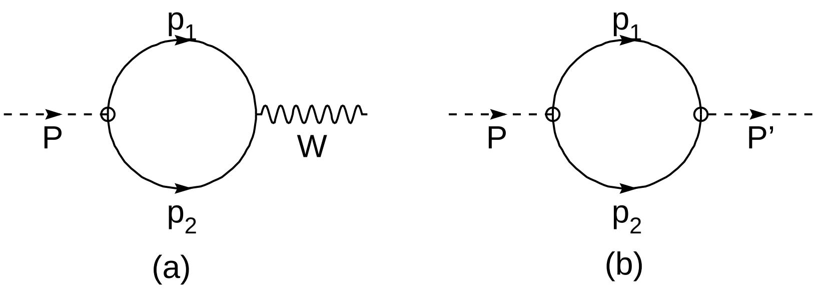

FIG. 2.

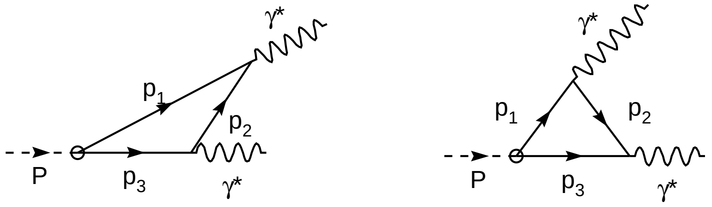

(a)

(b)

FIG. 3.

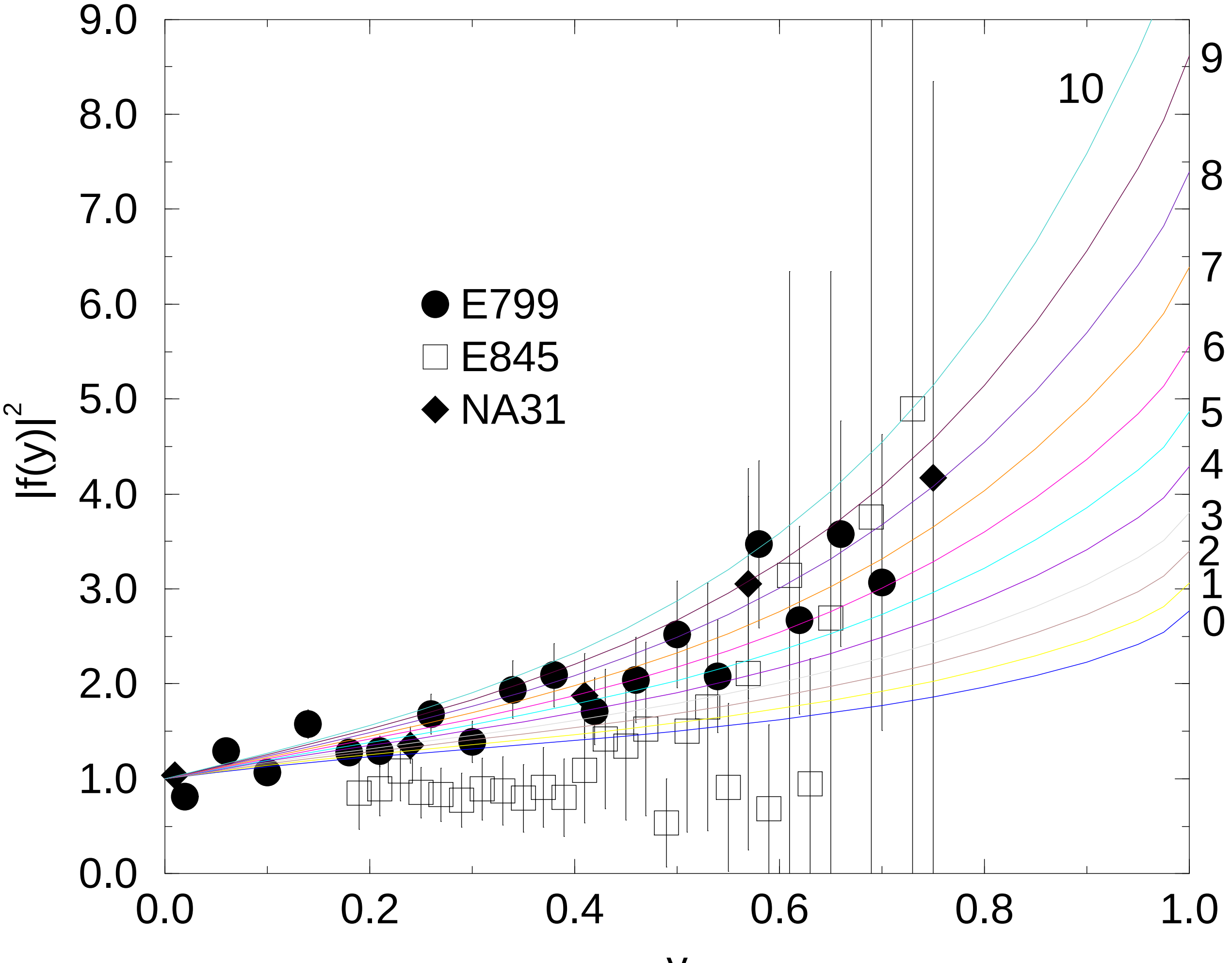

9.0
8.0
7.0
6.0
5.0
4.0
3.0
2.0
1.0
0.0
|f(y)|^2
0.0
0.2
0.4
0.6
0.8
1.0
y
● E799
☐ E845
◆ NA31
10
9
8
7
6
5
4
3
2
1
0